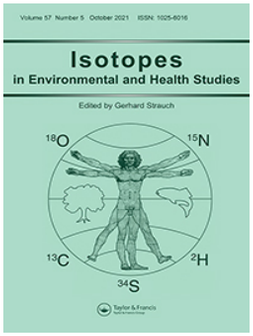

Isotopes in Environmental and Health Studies

ISSN: (Print) (Online) Journal homepage: https://www.tandfonline.com/loi/gieh20

Exploring the 2013–2018 degassing mechanism from the Pesje and Preloge excavation fields in the Velenje Coal basin, Slovenia: insights from molecular composition and stable isotopes

Tjaša Kanduč, Jerneja Sedlar, Rok Novak, Ivo Zadnik, Sergej Jamnikar, Timotej Verbovšek, Fausto Grassa & Janez Rošer

To cite this article: Tjaša Kanduč, Jerneja Sedlar, Rok Novak, Ivo Zadnik, Sergej Jamnikar, Timotej Verbovšek, Fausto Grassa & Janez Rošer (2021): Exploring the 2013–2018 degassing mechanism from the Pesje and Preloge excavation fields in the Velenje Coal basin, Slovenia: insights from molecular composition and stable isotopes, Isotopes in Environmental and Health Studies, DOI: 10.1080/10256016.2021.1981309

To link to this article: https://doi.org/10.1080/10256016.2021.1981309

Published online: 08 Oct 2021.

ISOTOPES IN ENVIRONMENTAL AND HEALTH STUDIES
https://doi.org/10.1080/10256016.2021.1981309

Exploring the 2013–2018 degassing mechanism from the Pesje and Preloge excavation fields in the Velenje Coal basin, Slovenia: insights from molecular composition and stable isotopes

Tjaša Kanduč[a], Jerneja Sedlar[b], Rok Novak[a], Ivo Zadnik[b], Sergej Jamnikar[b], Timotej Verbovšek[c], Fausto Grassa[d] and Janez Rošer[b]

[a]Department of Environmental Sciences, Jožef Stefan Institute, Ljubljana, Slovenia; [b]Velenje Coal Mine d.o.o., Velenje, Slovenia; [c]Department of Geology, Faculty of Natural Sciences and Engineering, University of Ljubljana, Ljubljana, Slovenia; [d]Istituto Nazionale di Geofisica e Vulcanologia Sezione di Palermo, Palermo, Italy

ABSTRACT

Gas samples were collected from 25 m long horizontal boreholes drilled into the excavation field at 10° inclination to the longwall face in two mining areas, Pesje and Preloge, in the Velenje Coal Mine, Slovenia, from 2013 to 2018. The degassing mechanism of coalbed gas and its stable isotopic composition ($\delta^{13}C_{CO2}$, $\delta^{13}C_{CH4}$, and $\delta^{2}H_{CH4}$) were investigated in boreholes in advance of eight working faces. The major coalbed gas constituents were CO_2 and methane. Gas concentrations and isotope values revealed that the methane is biogenic in origin with $\delta^{13}C_{CH4}$ values of −69.4 to −29.5 ‰, $\delta^{2}H_{CH4}$ values of −301 to −222 ‰, and a fractionation factor ($\alpha_{CO2\text{-}CH4}$) of 0.998–1.073, suggesting that methane derives from microbial acetate fermentation and CO_2 reduction. The carbon dioxide methane index values ranged from 50.0–98.3 vol.% and $\delta^{13}C_{CO2}$ values from −11.8 to −0.5 ‰, indicating that CO_2 is biogenic and endogenic in origin. The degassing mechanism results in isotope fractionation of methane and CO_2 for carbon isotopes up to 39.9 ‰ and up to 8.5 ‰, respectively, depending on the position of the excavation fields in space, e.g. under pre-mined coal area, fresh overburden.

ARTICLE HISTORY
Received 2 April 2021
Accepted 10 August 2021

KEYWORDS
Carbon-13; carbon dioxide; coalbed gas; excavation fields; gas composition; isotope geochemistry; methane; spatial distribution; Velenje Basin; Slovenia

1. Introduction

Coalbed gas is composed of hydrocarbons (methane, ethane, propane, butane) in variable concentrations (0–90 vol.%), CO_2 (0 to ≥ 99 vol.%) and minor amounts of N_2, O_2, H_2, N_2 and He [1]. The composition of coalbed gas and its isotopic composition ($\delta^{13}C_{CO2}$, $\delta^{13}C_{CH4}$ and $\delta^{15}N_{N2}$), which accumulates in the coal matrix, are related to the structural

CONTACT Tjaša Kanduč tjasa.kanduc@ijs.si Department of Environmental Sciences, Jožef Stefan Institute, Ljubljana, Slovenia

Supplemental data for this article can be accessed at https://doi.org/10.1080/10256016.2021.1981309.

and geological characteristics of the coal basin during its formation [2–6]. The three major sources of natural gases are biogenic, thermogenic, and abiogenic [7–8].

Biogenic fluids (methane, CO_2, N_2, H_2O, H_2S) are formed during early and late-stage diagenesis from the degradation of organic matter by microorganisms. Early-stage diagenesis includes all of the changes that occur during peat accumulation and burial up to 100 m, where temperatures have not yet increased, and where pores remain filled with water [9]. Most biogenic gases are formed as 'late stage' gases generated after the coalbeds are exhumed, exposed to the surface, or receive meteoric water recharge and nutrients from groundwater, which stimulates methanogenesis in the coal reservoir downslope. The formation of biogenic gas is limited to depths of up to $\geq$ 500 m temperatures < 50°C, and low salinity, but can occur in coals of all ages provided that it can be reached by the bacterial consortium. The diagenesis of organic matter (aerobic and anaerobic oxidation) is caused by microorganisms present in the water environment. In the absence of electron acceptors such as NO_3^-, Mn^{4+}, Fe^{3+} and SO_4^{2-}, Eh decreases, which leads to methane formation [10]. Methanogens are a group of anaerobic microorganisms that generate methane under strictly anaerobic conditions [11]. Bacteria and fungi perform the initial steps of biodegradation, followed by methanogenic *Archaea*, which then initiate the process of reducing complex organic structures: carbohydrates, proteins, and lipids, into simpler molecules such as acetic acid, CO_2 and H_2. Certain methanogens also consume acetate to generate CO_2 and CH_4, while others use hydrogen gas to reduce CO_2 [12–14]. In nature, biogenic methane is formed via two processes:

$$\text{Fermentation of acetate: } CH_3COOH \rightarrow CH_4 + CO_2 \tag{1}$$

$$\text{Reduction of } CO_2 \text{ to methane: } CO_2 + 8H^+ + 8e^- \rightarrow CH_4 + 2H_2O \tag{2}$$

Thermogenic gases (CO_2, CH_4, and N_2) are generated by the thermal cleavage of higher mass hydrocarbons and kerogen. In coal, most of the methane is generated by the thermal maturation of coal or during the coalification process, where small amounts of H_2S, N_2 and higher hydrocarbons are produced. The amount of these hydrocarbons is indicated by the gas wetness (C_{2+}) of the coal, i.e. the greater the number of higher hydrocarbons, the wetter the gas [15].

In groundwater that has low redox potential and in the absence of organic matter, methane can also form by the reduction of CO_2, e.g. from the weathering of mafic minerals and other natural abiotic reactions that form methane [14,16]:

$$15FeO_{(fo\text{-}en)} + 3H_2O + CO_2 \rightarrow 5Fe_3O_4 + H_2 + CH_4 \tag{3}$$

Gas–water–rock interactions, which do not directly involve organic matter, produce abiogenic gas [17]. Abiogenic methane has $\delta^{13}C$ values greater than −40 ‰, showing the absence of bacterial processes. Also, methane from the crust and the core is enriched with ^{13}C and has $\delta^{13}C$ values of −20 to −15 ‰. Carbon dioxide with $\delta^{13}C$ values of −10 to −5 ‰ [18] is characteristic of coalbed gas with high CO_2 values and a carbon dioxide methane index (CDMI $\leq$ 99 vol.%) typical for endogenous CO_2 related to fault activity. Gases are also generated by endogenous processes, including H_2O in the liquid and gas state and small amounts of CO, H_2, SO_2, H_2S, N_2, and CH_4 [18].

The characterization and isotopic composition of coalbed gas are used to determine the origin of its constituent gases and, importantly, for understanding and predicting gas

outbursts and stress build up in the seams [19]. The latter is important because tectonically deformed coal is more prone to gas outbursts [20]. Also, the dynamics of coal excavation in active coal mines is an important factor related to gas and rock outbursts [21].

Machine learning tools are becoming an increasingly important tool for deciphering the origin of methane. For example, revised genetic fields using a large dataset of 20,621 gas samples from 76 countries/territories and various geological habitats provide a modern standard for interpreting the origin of natural gases [3]. For this purpose, a machine learning tool with input parameters: $CH_4/(C_2H_6+C_3H_8)$, $\delta^{13}C_{CH4}$, $\delta^{2}H_{CH4}$, $\delta^{13}C_{CO2}$ was developed, which can determine the origin of gases in samples accompanied by an estimation of the model's accuracy and a confidence score for each possible origin [22].

The Velenje lignite was deposited earlier than gas genesis [23,24] from the biogeochemical decomposition of organic matter and has not undergone significant chemical changes [2]. The lignite is longwall mined underground at depths of around 500 m from seams that are subject to significant amounts of stress and coalbed gas emissions. For example, at the excavation field −65/E estimated gas emissions (measured at exit roadways) for methane and CO_2 were approximately 7.99 m^3/t for methane and 16.45 m^3/t for CO_2 (unpublished data), although emissions vary for each excavation field.

In this study, we report new data on coalbed gases (CO_2, CH_4, N_2), including carbon ($\delta^{13}C$) and hydrogen ($\delta^{2}H$) isotopic compositional data, $\alpha_{CO2\text{-}CH4}$ index values in advance of the working face and the spatial distribution of coalbed gases in the active excavation fields (2013–2018) of the Velenje Basin. Our aims are threefold:

To trace the degassing mechanism using concentration measurement and stable isotopic composition of carbon ($\delta^{13}C_{CO2}$, $\delta^{13}C_{CH4}$) in advance of the longwall faces active in 2013–2018.

To determine the origin of coalbed gases using concentrations of CO_2, methane, $\delta^{13}C_{CO2}$, $\delta^{13}C_{CH4}$, CDMI, $\alpha_{CO2\text{-}CH4}$ in the period 2013–2018.

To update existing GIS models of coalbed gases data from 2013–2018.

2. The Velenje basin

2.1. Geology of the Velenje Basin

The Velenje Basin lies in the northeastern part of Slovenia (Figure 1) at the junction of the WNW–ESE-trending Šoštanj fault and the E–W-trending Periadriatic fault zone, which is bounded in the south by the Smrekovec fault segment (Figure 1, Figure S1). The Šoštanj and Smrekovec faults exhibit strike-slip and younger oblique-slip movement due to compression generated by the collision of the continental plates. On the NE side of the Velenje fault in the pre-Pliocene basement, Triassic limestones and dolomites dominate, while Oligocene to Miocene clastic strata, consisting predominantly of marls, sandstones and volcanoclastic sediments, dominate in the SW [25]. In the lower part of the lower Triassic (Scythian layers) region, anhydrite is present, while the upper part consists of gray stratified dolomite, which transitions toward the top into unstratified dolomite of Anisian age [26]. The basin fill has an estimated thickness of ∼1000 m (Figure S1). The pre-Pliocene basement is formed of Late Paleozoic (shales, quartz, limestone and breccia), Triassic (dolostones, shales, limestones), Eocene (marls, sandstones, siltstones with coal occurrence) and Miocene rocks (sandstones, conglomerates, marls). Below the main lignite seam (160 m

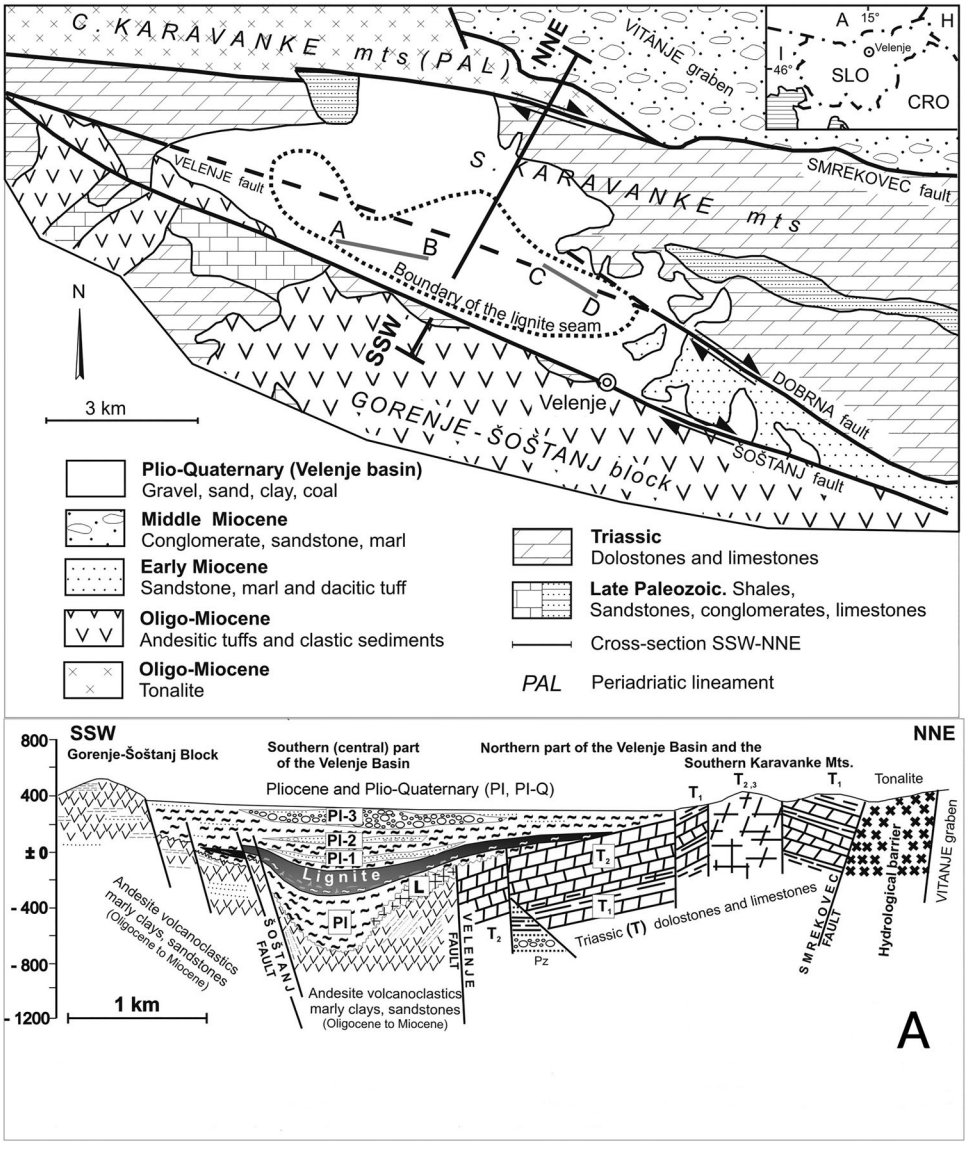

Figure 1. Geological map of the Velenje Coal Basin with schematic geological cross-section NNE – SSW of the Velenje Basin, adapted from [24, 31, 32] and hydrogeological profiles A–B and C–D published in [35].

thick) are Pliocene and sandy–silty sediments with coarse clastics. Above this seam are Pliocene marls, claystones, massive claystone and sands, silts and sands, Quaternary green and yellow sandy silts and recent sands and gravels (Figure S1).

2.2. Velenje Longwall Mining Method (VLMM)

The average annual production of lignite in the Velenje Coal Mine is about 3.5 million tons per year. The lignite is mined using the Velenje Longwall Mining Method (VLMM), a longwall top coal caving method based on the retreating mining method. It is specific for the

Velenje coal seam, owing to its top coal caving heights (up to 15 m) and extraction of the lignite in front of the hydraulic shields [27]. The rate at which the lignite can be excavated using this method depends on several factors, one of which is the amount of coalbed gas released since high advancement rates (> 9 m per day) significantly increase the risk of gas outbursts [28–30].

2.3. Previous investigations of coalbed gases in the Velenje Coal Mine

Geochemical monitoring of coalbed gases (molecular and isotopic characteristics) and the advancing rate of the working face was established by the Jožef Stefan Institute (JSI) and the Velenje Coal Mine Company in the year 2000. Since then, 119 coalbed gas samples from excavation fields were entered into the GIS environment to present geochemical data in space [30]. The studies revealed that major gas components were CO_2, methane and N_2 in lower concentrations.

In 2016, 2017 and 2018, new boreholes (Figure 2) were drilled (JPK 83+10°, JPK 89+10°, JPK 91+10°) and new coalbed gas data were obtained.

This time, temporal changes in the chemical and isotopic composition of free seam gases were observed within the boreholes as a function of the advancing working face [28–30]. These studies revealed that at a distance of around 120 m from the working face, the influence of coal exploitation by the VLMM causes coalbed gas to migrate

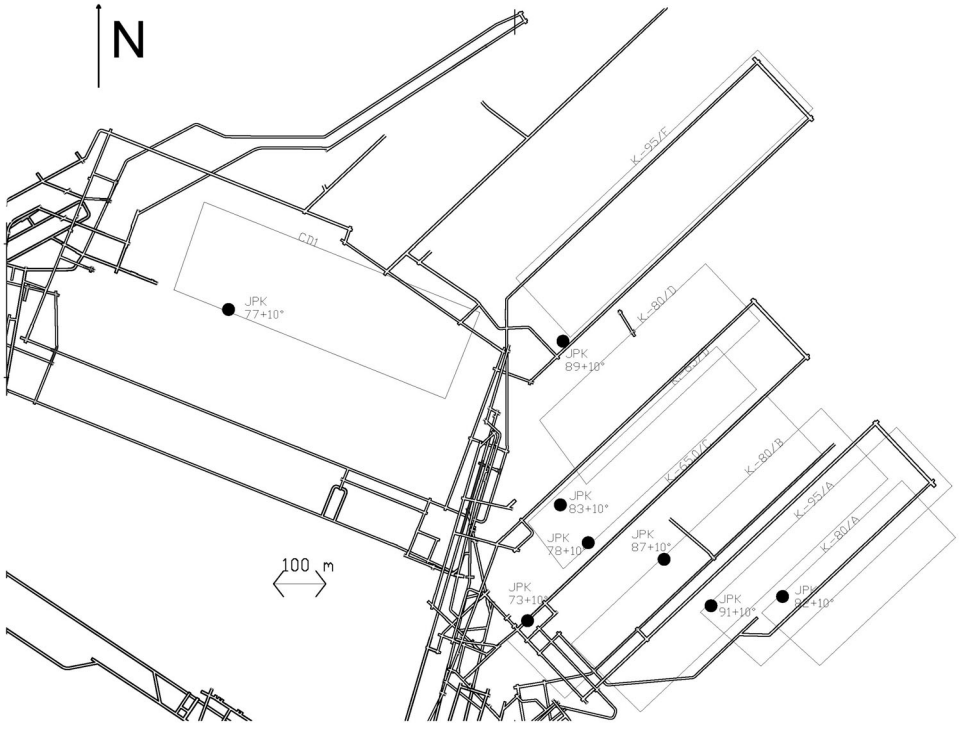

Figure 2. Sampling locations: K.–65/C, K.–65/D, CD/1, K.–80/A, K.–80/B, K.–80/D, K.–95/E, K.–95/A and boreholes JPK 73+10°, JPK 78+10°, JPK 77+10°, JPK 82+10°, JPK 87+10°, JPK 83+10°, JPK 89+10°, JPK 91+10° drilled in 2013–2018.

through the cracks in the crushed structure. At 30–70 m, the crushing of the lignite structure, causes previously fixed CO_2 to desorb from the coal matrix.

The $\delta^{13}C_{CH4}$ values revealed that at shallower depths (G2/C, K.−50/C, K.−130/A, K.–5/A), the lignite has lower $\delta^{13}C_{CH4}$ values, suggesting a biogenic origin, whereas at deeper levels, the $\delta^{13}C_{CH4}$ values are higher, indicating thermogenic origin [27]. Gas composition and isotopic studies also identified endogenic CO_2 and both biogenic CO_2 and methane [27,31-33]. However, although the higher $\delta^{13}C_{CH4}$ values could also be attributed to migration processes during coal excavation [34], the isotope fractionation resulting from degassing during excavation remains poorly investigated.

2.4. Isotopic composition of methane and CO_2 in Velenje Basin in the period 2013–2018

We compared the $\delta^{13}C_{CH4}$ and $\delta^{13}C_{CO2}$ values of the Velenje samples (2013–2018) with different environmental matrixes, e.g. petroleum, plants, and microbial methane (Figure 3). The Vienna Pee Dee Belemnite has a default δ value of 0 ‰ [38]. Biogenic methane is enriched with the light ^{12}C isotope, while methane associated with petroleum is enriched in ^{13}C isotope and deep sourced CO_2 has values around −7 ‰ (Figure 3). Also, C_3 plants have $\delta^{13}C$ values from −30 to −20 ‰, while C_4 plants have $\delta^{13}C$ values between −18 and −10 ‰ (Figure 3).

3. Materials and methods

In previous studies (2000–2018), both free and coalbed gases were analyzed, including volatile gases present in pores and cracks within the lignite structure and evolved gas

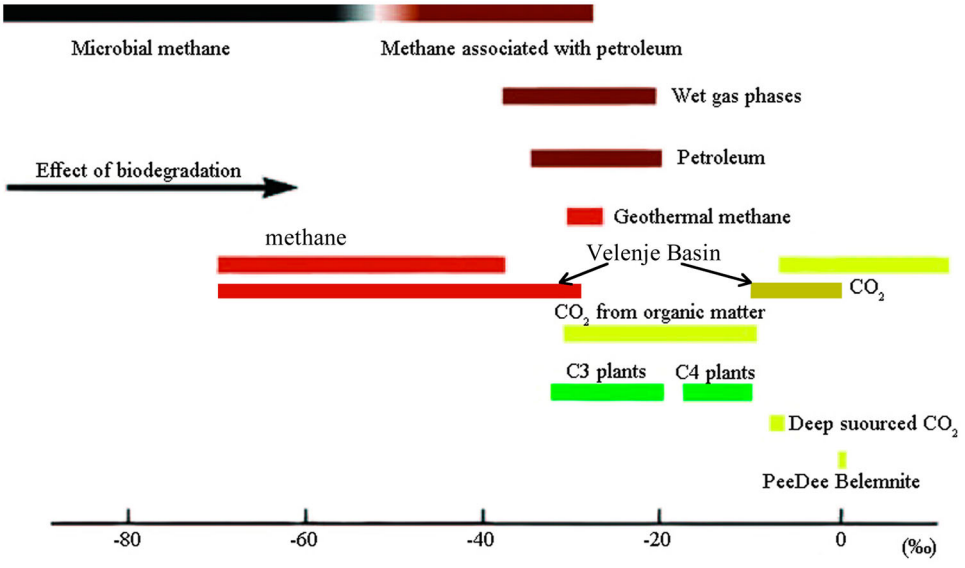

Figure 3. Carbon isotope signatures from different sources [39] and $\delta^{13}C_{CO2}$ and $\delta^{13}C_{CH4}$ values for the Velenje Basin (2013–2018).

during drilling [40]. The origin of coalbed gas was determined using mass spectrometry. Horizontal boreholes (3–25 m) were drilled to monitor coalbed gases and their isotope values. Two boreholes were drilled at each excavation field at an inclination +2 and +30° into the longwall panel (2000–2013). A GIS model of the coalbed gas data and isotope values for methane and CO_2 had already been established based on 2000–2015 data: however, only intact samples were used in the model due to suspected gas migration.

In the present study, coalbed gas was sampled at the following working faces (Figure 2): K.−65/C (JPK 73+10°), n = 36, K.−65/D (JPK 78+10°), n = 15, CD/1 (JPK 77+10°), n = 8, K.−80/A (JPK 82+10°), n = 23, K.−80/B (JPK 87+10°), n = 20, K.−80/D (JPK 83+10°), n = 26, K.−95/E (JPK 89+10°), n = 17, K.−95/A (JPK 91+10°), n = 6 (Figure 2). One borehole was drilled at each excavation field at an inclination of +10° to the horizontal longwall panel. Altogether, 151 samples were collected during 2013–2018 at eight excavation fields and analyzed to obtain gas concentrations and $\delta^{13}C_{CO2}$ and $\delta^{13}C_{CH4}$ data.

The design of the boreholes (since 2000) is described in detail in [27]. All boreholes (25 m x 101 mm ø) were drilled at active mine sites. A steel casing (20 m x 85 mm ø) was then inserted into the boreholes, and inside this casing was installed a 25.4 mm polyethylene tube with the last 5 m perforated. Sealant foam was used to seal the polyethylene casing to the depth of 20 m. Inside the polyethylene tubing was a capillary copper sampling tube (ø = 2 mm) and an auxiliary copper sampling tube (ø = 6 mm) [27].

Coalbed gas was then collected using a 50 mL plastic syringe and transferred to a 12 mL Labco glass ampoule fitted with a gas-tight septum, flushed using two needles (input and output needle) and filled with coalbed gas under pressure. Seven ampoules were filled at each location and stored at standard atmospheric conditions until analysis.

Contamination with the mine's ventilation air meant that samples were calculated on an air-free basis. Based on the N_2:O_2 ratio in air the percentage of nitrogen in the samples was calculated based on the amount of oxygen present in the ampoules and Dalton's law [41]. As a result, nitrogen (N_2) was found to be in excess at the following excavation fields: K.−65/C (10 samples), K.−65/D (6 samples), CD/1 (5 samples), and K.−80/B (10 samples).

The concentrations of CH_4, CO_2, N_2, O_2 and Ar were determined using a custom-made NIER mass spectrometer at the Jožef Stefan Institute. Singular value decomposition of the matrix was used to allow simultaneous analysis of the gases (method precision was ± 3%, Table S9). Before 2013 the isotopic compositions of methane and CO_2 were determined at the JSI using a Europa 20–20 continuous flow isotope ratio mass spectrometer (IRMS) fitted with an ANCA-trace gas (TG) preparation module (Sercon Ltd., Cheshire, UK). First, water was removed, and the CO_2 was directly analyzed for $\delta^{13}C_{CO2}$. For CH_4 measurements, CO_2 was removed and the CH_4 combusted over hot 10 % platinum CuO (1000 °C). The CH_4 once converted to CO_2 was then analyzed directly to obtain its isotopic composition ($\delta^{13}C$). Working standards calibrated to the International Atomic Agency (IAEA) reference materials were used to obtain known $\delta^{13}C_{CO2}$ and $\delta^{13}C_{CH4}$ values: Messer Austria GmbH with $\delta^{13}C$ = -35.4 ±0.2 ‰ and laboratory working standard with a value of −5.2 ±0.2 ‰ for $\delta^{13}C_{CO2}$ was used together with working standards with $\delta^{13}C$ values of −47.5 ±0.6 ‰ and −53.4 ±0.6 ‰ for methane. The analytical precision was ±0.2 ‰ for CO_2 and ±0.6 ‰ for CH_4.

After 2013 the concentrations of coalbed gases and the $\delta^{13}C_{CH4}$ and $\delta^{13}C_{CO2}$ values were determined by the Institute Nazionale di Geofisica e Vulcanologia Sezione di Palermo in Italy. In both sampling periods, 2000–2013 and 2013–2018, mass spectrometry was used to determine the origin of coalbed gases producing comparable results. In addition, a comparison of stable isotope results between both labs was performed in 2013–2015. Differences between laboratories was for $\delta^{13}C_{CH4}$ 1.9 ‰ and for $\delta^{13}C_{CO2}$ 0.5 ‰.

Permanent gases (CO_2, CH_4 and N_2) were determined using a gas chromatograph (GC, Agilent 7890 equipped with PPU and MS5A columns) fitted with a MicroGC module (equipped with a PPU column) and a double detector (TCD and FID) using argon as the carrier gas. Analytical precision was >±5 % for all the gas species. The isotope analyses ($\delta^{13}C_{CO2}$, $\delta^{13}C_{CH4}$, $\delta^{2}H_{CH4}$) were performed using a Thermo Delta Plus XP IRMS (Isotope Ratio Mass Spectrometer) equipped with a Thermo TRACE GC interfaced with Thermo GC/C III (for carbon) and a Thermo GC/TC (for hydrogen). Separation was achieved on a Rt-Q Plot column (Restek 30 m X 0.32 mm i.d.). The oven programme was isothermal: 50°C for carbon and 40°C for hydrogen. The carrier gas flow rate (He of 5.6 grade) was kept at a constant 0.8 cc min^{-1}. The injection system is described in detail in [42]. Injections were performed in the split mode using a split ratio of 10:1–80:1. Methane was converted quantitatively to CO_2 in a combustion oven (T= 940°C) or H_2 in a reactor at 1440°C.

Each sample analysis took about eight minutes. The accuracy and precision of the method were examined using a standardized gas. The external analytical precision (1σ) was < 0.1 ‰ for the $^{13}C/^{12}C$ ratios (both CO_2 and CH_4) and 1 ‰ for the $^{2}H/H$ ratios, calculated from 10 repeated analyses of the same sample. Stable isotopes are reported in the δ notation [38]. The two internal reference CO_2 gases (Naftia $\delta^{13}C = -0.89$ ‰ and SOL $\delta^{13}C = -28.45$ ‰) were calibrated to the NIST CO_2 international gas reference standard RM8564 ($\delta^{13}C = -10.45$ ‰), while for methane, an internal pure CH_4 reference ($\delta^{13}C = -49.5$ ‰), calibrated against two reference materials B-ISO 1 and T-Iso 1 (Isometric instruments) was used. Two-point and one-point normalization was performed for CO_2 and methane, respectively.

The relative difference of isotope ratios (also called relative isotope-ratio or delta values) has been reported using the short-hand notation $\delta^{i/j}E$. The isotope –delta value is obtained from isotope number ratios $R(^{i}E, ^{j}E)_p$ as follows [43]:

$$\delta(^{i,j}E) = \delta^{i,j}E = \frac{^{i/j}R_p - ^{i/j}R_{Ref}}{^{i/j}R_{Ref}} \tag{4}$$

where ^{i}E denotes the higher (superscript i) and ^{j}E the lower (superscript j) atomic mass number of element E. The subscript P denotes the substance used to determine the respective values, $R(^{i}E, ^{j}E)_p$ is isotope number – ratios.

Fractionation factor α is used to distinguish between CH_4 generated via CO_2 reduction and acetate fermentation [44]. Whiticar et al. [12] suggested that variations in carbon isotope fractionation (α) between CO_2 and CH_4 could be utilized to distinguish between CH_4 generated via CO_2 reduction and acetate fermentation as follows:

$$\alpha^{13}C_{CO2-CH4} = (\delta^{13}C_{CO2} + 1000)/(\delta^{13}C_{CH4} + 1000) \tag{5}$$

The CDMI was introduced to evaluate higher CO_2/lower CO_2 concentrations at excavation fields [29] and is calculated as follows:

$$CDMI = (CO_2/(CO_2 + CH_4)) \cdot 100\% \quad (6)$$

Statistical analysis was conducted using the R language [45]. Principal component analysis (PCA) and hierarchical clustering analysis (with dendrogram) were used to group coalbed gas samples collected from the excavation fields (K.−65/C, K.−65/D, CD/1, K.−80/A, K.−80/B, K.-80/D, K.−95/E, and K.−95/E). The principal component biplots were made using the ggplot2 package [46], and the dendrogram was constructed using the R package factoextra. Only complete cases were considered for clustering and PCA (starting a dataset of 155 observations, reduced to 121 observations after excluding incomplete observations).

Euclidean distances were calculated to construct the dendrogram, while Ward's Minimum Variance algorithm was used as the clustering method, where groups are formed so that the within-group sum of squares is minimized. For PCA, the prcomp function in R was used, with centering (mean zero) and scaling (unit variance). In the case of missing data (e.g. distance from the longwall face, $\delta^{13}C_{CH4}$, $\delta^{2}H$), samples were excluded from PCA analyses.

A free web-based machine learning tool [47] was used to determine the origin of natural gases. If one of the input parameters ($\delta^{13}C_{CH4}$, $\delta^{13}C_{CO2}$, and $\delta^{2}H_{CH4}$) to the machine learning tool was missing, the model accuracy was <90 % (Tables 1–8).

4. Results

The CO_2 in the Velenje Basin samples (2013–2018) is partly from organic matter and partly from deep sourced CO_2, while the methane is primarily of microbial origin (Figure 3).

All results from the active excavation fields: K.−65/C, K.−65/D, CD/1, K.−80/A, K.−80/B, K.-80/D, K.−95/E, K.−95/A are presented in the (Tables S1–8), while results of CO_2, CH_4, CDMI, $\delta^{13}C_{CO2}$, $\delta^{13}C_{CH4}$ and $\alpha_{CO2\text{-}CH4}$ were used to the GIS maps Table S9.

Results show that the main coalbed gas components were $CO_2 > CH_4 > N_2$ at the following working faces: K.−65/C, K.−65/D, CD/1, and K.−80/B (Tables S1–8). Ranges of measured and calculated parameters: CDMI, $\delta^{13}C_{CO2}$, $\delta^{13}C_{CH4}$, $\delta^{2}H_{CH4}$, $\alpha_{CO2\text{-}CH4}$ from excavation fields: K.−65/C, K.−65/D, CD/1, K.−80/A, K.−80/B, K.−80/D, K.−95/E, K.−95/A are presented in Table 1.

The most significant variations in $\delta^{13}C_{CH4}$ and $\delta^{2}H_{CH4}$ were observed in K.−80/A (Tables S1 and S4). The CDMI ranged from 50 to 98.3 vol.%, with the broadest range of CDMI values observed at K.−80/A (Pesje), while CDMI values of 50.0–98.3 vol.% suggest that CO_2 is the major component of coalbed gas (Table 1). The $\delta^{13}C_{CO2}$ values range from -11.8 to −0.5 ‰, and $\delta^{13}C_{CH4}$ values from −69.4 to −29.5 ‰ (Table 1). The broadest range of $\delta^{13}C_{CH4}$ values (−69.4 to −29.5 ‰) and $\delta^{2}H_{CH4}$ values (−301 to −222 ‰) were observed at K.−80/A. Here, the $\alpha_{CO2\text{-}CH4}$ values ranged from 0.990–1.073.

The calculated gas dryness index ($C_1/(C_2+C_3)$) was determined at K.−130/B, G3/C, K.−65/F in the previous study [27] and ranged between 339.74 and 23272.7 ppm. The concentrations of higher hydrocarbons investigated ranged as follows: ethane from 0 to 122 ppm, propane from 0 to 158 ppm, iso-butane from 0 and −15.3 ppm, *n*-butane from 0 to 7.6 ppm, iso-pentane from 0 to 12.2 ppm, *n*-pentane from 0 to 5 ppm,

Table 1. Ranges of CDMI, $\delta^{13}C_{CO2}$, $\delta^{13}C_{CH4}$, $\delta^{2}H_{CH4}$, $\alpha_{CO2\text{-}CH4}$ from excavation fields K.−65/C, K.−65/D, K. CD/1, K.−80/A, K.−80/B, K.−80/D, K.−95/E, K.-95/A.

Excavation fields	CDMI (%)	$\delta^{13}C_{CO2}$ (‰)	$\delta^{13}C_{CH4}$ (‰)	$\delta^{2}H_{CH4}$ (‰)	$\alpha_{CO2\text{-}CH4}$
K.-65/C	53.8 to 94.3	−9.6 to −8.4	−56.7 to −46.7	−326 to −293	1.040 to 1.046
K.-65/D	52.9 to 85.7	−11.8 to −3.3	−58.3 to −53.4	−320 to −285	0.990 to 1.058
K. CD1	50.9 to 66.8	−8.5 to −7.7	−55.7 to −53.7	−306 to −281	1.048 to 1.051
K.-80/A	80.0 to 97.6	−4.6 to −1.2	−69.4 to −29.5	−301 to −222	0.998 to 1.073
K.-80/B	50.0 to 90.2	−9.8 to −4.2	−47.5 to −31.4	−357 to −301	1.000 to 1.044
K.-80/D	50.0 to 76.9	−10.3 to −9.2	−41.3 to −33.5	−341 to −326	1.024 to 1.033
K.-95/E	95.5 to 98.3	−8.2 to −7.6	−45.4 to −37.3	−357 to −326	1.031 to 1.039
K.-95/A	83.5 to 85.1	−8.3 to −0.5	−67.7 to −35.4	−331 to −301	0.995 to 1.074

and hexane from 0 to 21 ppm. In this case, coalbed gas was treated as a dry gas since methane is prevalent [27].

5. Discussion

5.1. Mechanism of degassing from excavation fields: concentrations of coalbed gases (CO_2 and CH_4) and stable isotopic composition of carbon in CO_2 ($\delta^{13}C_{CO2}$) and methane ($\delta^{13}C_{CH4}$)

The relations between degassing from excavation fields and the isotopic composition of carbon are still poorly investigated. Therefore, we focused on the relations between CO_2 and methane, $\delta^{13}C_{CO2}$ and $\delta^{13}C_{CH4}$, and longwall face speeds (Table 3).

Table 2 gives the position of excavation field in space and velocity rates in advance of the working faces for K.−65/C, K.-65/D, CD/1, K.−80/A, K.−80/B, K.−80/D, K.−95/E, K.-95/A.

Generally, high CO_2 values coincide with low methane concentrations, a pattern that is observed at all longwall faces (Figure 4 A, Figure S2 A, B, D), except at K.−80/A, K.−80/D, K.−95/E and K.−95/A, where the gas concentrations are constant (Figure S2 C, E–G). At all other excavation fields, variations in the CO_2 and methane content were observed in advance of the working face. This is because coal excavation also results in secondary fissures, which releases the coalbed gas stored in the pores of the coal reservoir.

The rate (m/day) at which the working face progresses towards the boreholes was also investigated since higher extraction rates (9 m/day or more) can trigger coalbed gas outbursts, especially since concentrations of CO_2 and methane can vary significantly in

Table 2. Position of excavation field in space and velocity of the active working faces (2013–2018).

Excavation field	Activity	Position of excavation field in space	Velocity (m/day)
K.−65/C	November 2013–October 2014	Partly under fresh overburden	0.5 to 4.0
K.−65/D	October 2014–March 2015	Fresh overburden	1.8 to 4.0
K. CD/1	July 2014–March 2015	Fresh overburden	1.2 to 3.1
K.−80/A	April 2015–September 2015	Under pre-mined coal area	0.5 to 3.0
K.−80/B	September 2015–May 2016	Partly under fresh overburden	0.4 to 3.3
K.−80/D	September 2016–May 2017	Under fresh overburden and under pre-mined coal area	0.0 to 3.6
K.−95/E	July 2017–March 2018	Partly under fresh overburden	0.7 to 5
K.−95/A	February 2018–October 2018	Under pre-mined coal area	1.3 to 2.1

advance of the working face [29]. At the Velenje Mine in this period, the velocity of the working face at active excavation fields was not allowed to exceed 5 m/day (Table 2) for safety reasons.

A complex situation of the stress state occurs during the excavation of lignite where a dynamic wave is created, whose shape depends on excavation and geomechanical conditions in the excavation pillar. The higher the advancement rate, the closer the stress wave is to the working face [48, 49], which can affect the levels of CO_2 and methane [27]. The effects of changing stress were investigated by installing a tri-axial cell in the lignite structure. Results show that at a distance of 120 m from the working face, vertical stresses increase. At a distance of 80 m, shearing and tearing of the lignite structure occurred and, vertical stresses increased, while horizontal and transverse stresses decreased. At 30–50 m from the tri-axial cell, the vertical stresses are so high that the lignite structure collapses. Besides stress, the location of the excavation field in space is also important (Table 2).

At K.−65/C at a distance of 110 m from the longwall face, methane levels increased while levels of CO_2 decreased (Figure 4). A maximum methane concentration occurs at 66 m, which coincides with a minimum CO_2 level (Figure 4). The lignite is crushed at a distance of 11 m, and while CO_2 remains adsorbed, methane escapes (Figure 4). Here the excavation field is located partly under fresh overburden and the $\delta^{13}C_{CO2}$ values remain relatively constant ($\delta^{13}C_{CO2}$ ranges from −9.6 to −8.4 ‰) with distance from the longwall face, while $\delta^{13}C_{CH4}$ values increase (−56.7 to −46.7 ‰). A shift in both $\delta^{13}C_{CO2}$ and $\delta^{13}C_{CH4}$ values is observed at a distance of 30 m from the longwall face (Figure 4). At 120 m from the longwall face, whereas the $\delta^{13}C_{CH4}$ values decrease but then increase at 11 m when the lignite structure collapses. The $\delta^{13}C_{CO2}$ value also

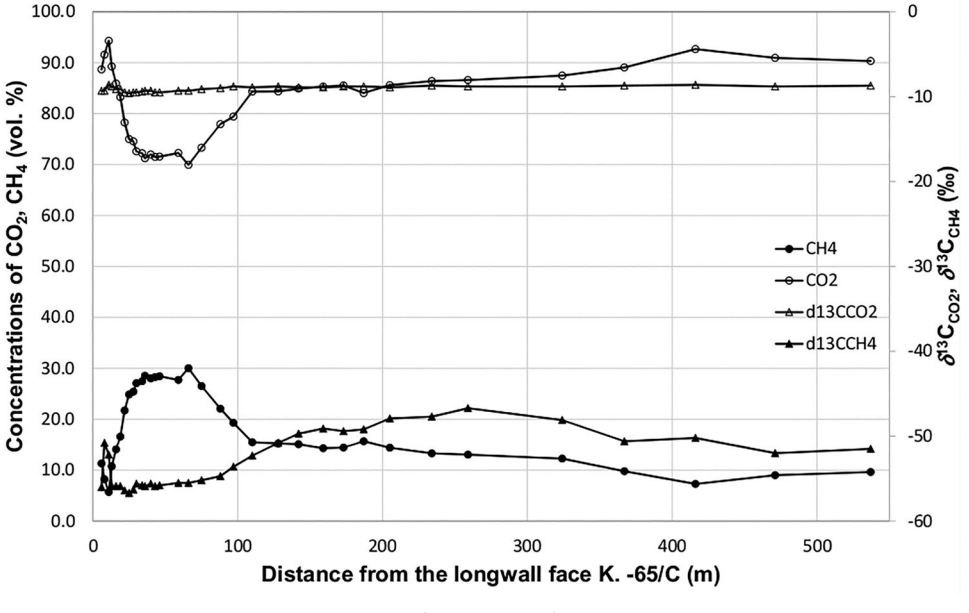

Figure 4. Methane, CO_2 concentrations, $\delta^{13}C_{CO2}$ and $\delta^{13}C_{CH4}$ with distance from the longwall face K.−65/C.

increases at a distance of 11 m from the working face. The mechanism of degassing of coalbed gases from other investigated excavation fields: K.−65/D, CD/1, K.−80/A, K.−80/B, K.−80/D, K.−95/E and K.−95/A are presented in the supplementary material (Figure S2).

Generally, two peaks in CO_2 occur, one at 120–180 m and a second 60–80 m from the longwall face. At 10–30 m the lignite structure collapses. Concentrations of CO_2 and methane with distance from the longwall either remain constant or a single peak is observed (60 m or 30 m) under pre-mined coal area, while under fresh overburden, two peaks of CO_2 and methane were detected. Significant variations in the $\delta^{13}C_{CH4}$ values (2–39.9 ‰) were observed with distance from the longwall face, while variations in $\delta^{13}C_{CO2}$ values were much smaller (0.6–8.5 ‰). This difference is because the effect of isotope fractionation is more pronounced for methane than CO_2. A decrease in the $\delta^{13}C_{CH4}$ values (as the lighter isotope ^{12}C escapes) is observed at 80–120 m from the longwall face, but then an increase is observed at 11 m as the lignite structure collapses. The degassing mechanism of CO_2 and methane is more expressed at longwall faces under fresh overburden, albeit no clear trends are observed at excavation fields located partly over fresh burden and pre-mined coal areas.

A good correlation (R^2 = 0.998) was obtained between methane and CO_2 concentrations at K.−65/C, K.−65/D, CD/1, K.−80/A, K.−80/B, K.−80/D, K.−95/E, and K.−95/A (Figure 5). Only specific gas samples from CD/1 and K.−65/D deviated from the regression line. Also, a similar good correlation was observed by [35], which is consistent with the physical and chemical properties of CO_2 and methane, i.e. methane migrates faster, while CO_2 adsorbes on coal [41].

5.2. Origin of CO_2

High CDMI and values of endogenic CO_2 (approx. −7 ‰) are characteristic only for K.−95/E, which is located partly under fresh overburden. Samples with a high CDMI and CO_2 reduction process are observed at K.−80/A, K.−80/D, and K.−95/A, located under pre-mined coal areas. Here, the CO_2 samples are enriched with ^{13}C (−4.6 to −1.2 ‰). The $\delta^{13}C_{CO2}$ values range from −8.3 to −0.5 ‰ at K.−95/A, indicating a mixture of endogenic and biogenic CO_2 (Figure 6). Samples from K.−95/E reveal high CDMI and $\delta^{13}C_{CO2}$ values of endogenic CO_2. The fields K.−80/D, CD/1, K.−65/D reveal a mixture of endogenic CO_2 and microbial CO_2 with a CDMI from 50 to 80 vol.% (Figure 6). Samples from K.−65/C indicate a high CDMI generally above 65 vol.%. Both CD/1 and K.−95/E are located under a fresh overburden and have a CDMI between 50–75 vol.% (Table 2, Figure 6). In this case, the CDMI is expected to be lower. Samples from K.−80/B (located partly under fresh overburden) indicate a reduction in CO_2 and a CDMI of $\leq$ 25 vol.%. Generally, a high CDMI is related to pre-mined coal areas, while a lower CDMI is related to excavation fields with fresh overburden.

5.3. Origin of methane

Among biogeochemical processes, CO_2 reduction prevails at K.−80/A (located under pre-mined coal area), while at CD/1, K.−65/C, K.−65/D, K.−80/B, K.−95/A, K.−80/D acetate fermentation is the major biogeochemical process (Figure 7 A). The fact that methane in one

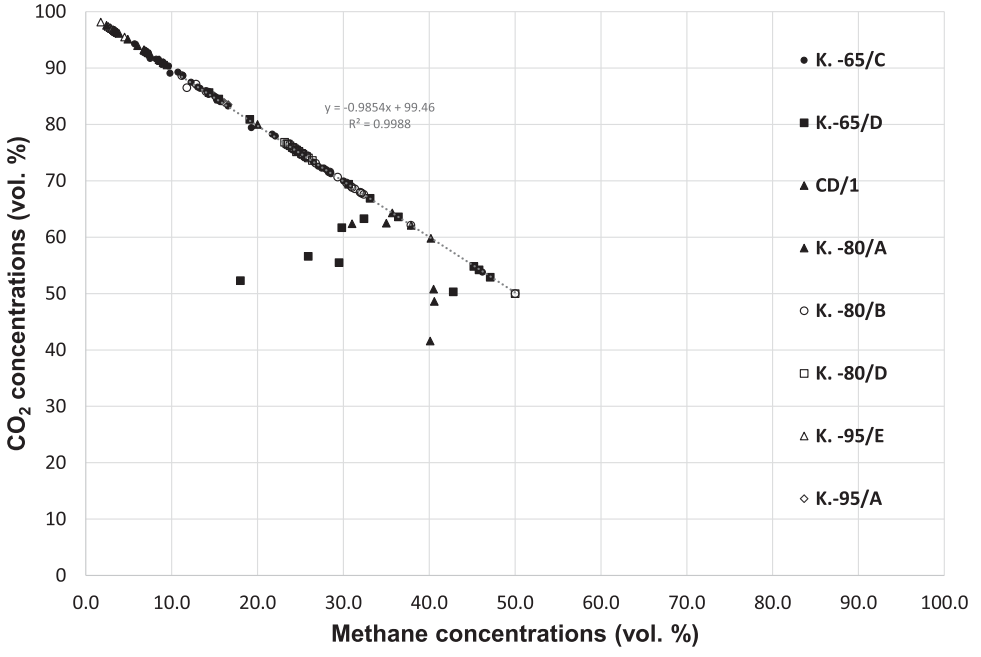

Figure 5. Plot of CO_2 versus methane concentrations.

sample from K.−80/A is acetate fermentation in origin and one sample from K.−80/A indicates CO_2 reduction with a high $\delta^{13}C_{CH4}$ value of about −30 ‰ and can be considered thermogenic in origin. At K.−80/A, K.−95/A values of $\delta^{13}C_{CH4}$ and $\delta^{2}H_{CH4}$ indicate microbial CO_2 reduction and endogenic CO_2 (Figure 7 B). Both K.−80/A and K.−95/A

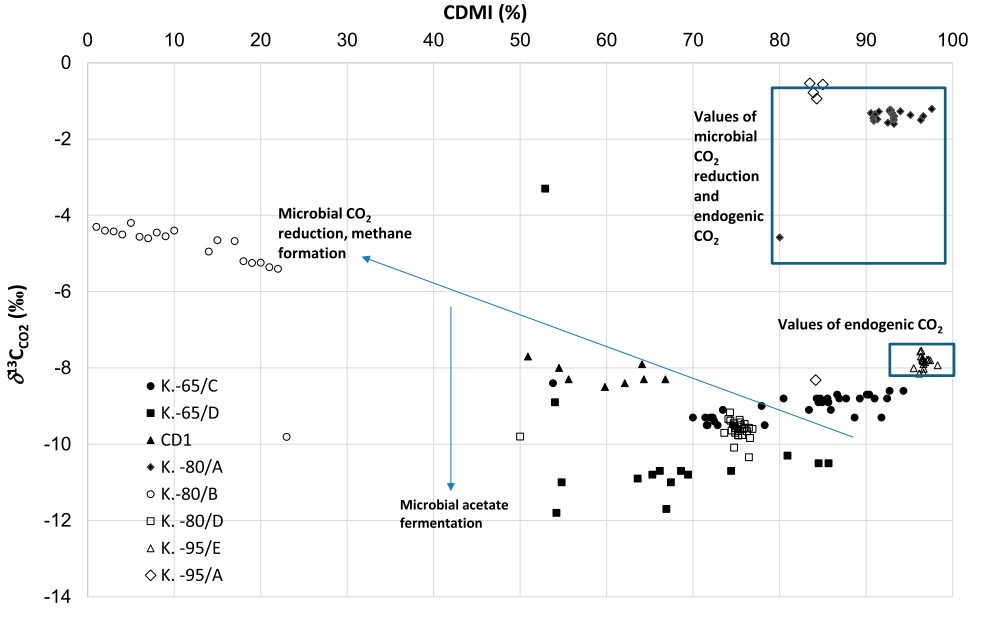

Figure 6. Plot of $\delta^{13}C_{CO2}$ versus CDMI.

have the most negative $\delta^{13}C_{CH4}$ values and are located under pre-mined coal. All other fields (K.–65/C, K.–65/D, CD/1, K.–80/B, K.-80/D, and K.–95/E) are located under fresh overburden or partly under fresh overburden and have more positive $\delta^{13}C_{CH4}$ values (Figure 7 A).

The differentiation between acetate fermentation and CO_2 reduction is shown in Figure 7 B. The fractionation lines $\alpha_c = 1.090$, $\alpha_c = 1.055$ and $\alpha_c = 1.044$ are proposed in [44]. Samples falling between lines $\alpha_c = 1.090$, $\alpha_c = 1.055$ indicate CO_2 reduction, while samples between lines $\alpha_c = 1.055$ and $\alpha_c = 1.044$ indicate acetate fermentation. The results show that K.–80/A and K.–95/A belong to acetate fermentation and CO_2 reduction, while CD/1, K.–65/, K.–65/D, K.–95/E, K.–80/B and K.–80/D belong to microbial acetate fermentation. The majority of the methane is biogenic in origin (Figure 7 A and B).

5.4. $\delta^{13}C_{CO2}$ and $\delta^{13}C_{CH4}$ versus depth

Previous studies showed that biogenic and thermogenic gases are depth and temperature-related [50]. Therefore, it would be expected that in deeper excavation fields there would be more thermogenic methane (enriched with ^{13}C), while at shallower depths, there should be more biogenic gas (enriched with ^{12}C). The isotopic composition of CBM (Coalbed Methane) from pilot and production wells from the northern Bowen Basin revealed that methane was enriched with ^{12}C at a depth of 100 m, while at 900 m methane was enriched with ^{13}C, although no clear trend in the $\delta^{13}C_{CO2}$ values was observed [51]. The relation between $\delta^{13}C_{CH4}$ and $\delta^{13}C_{CO2}$ values with depth in the Velenje Basin are shown in Figs. 8 A, B.

The average $\delta^{13}C_{CH4}$ values are as follows: K.–80/D (−37.0 ‰), K.–80/B (−37.4 ‰), K.–95/E (−40.6 ‰), K.–65/C (−52.9 ‰), CD/1 (−54.6 ‰), K.–65/D (−55.1 ‰), K.–80/A (-66.6 ‰), K.–95/A (−61.8 ‰). The difference in depth between excavation fields is 33.1 m. The deepest excavation field investigated in this study is K.–95/E ($\delta^{13}C_{CH4}$ = −40.6 ‰), and the shallowest is K.–65/C ($\delta^{13}C_{CH4}$ = −52.9 ‰) (Figure 8 A and B). The $\delta^{13}C_{CH4}$ values (Figure 8 A) are enriched with ^{13}C at deeper excavation fields: K.–95/E (all samples), K.–95/A (one sample), K.–80/D (all samples) and K.–80/B (all samples), and K.–80/A (one sample). The shallower fields: K.–65/C, and K.–65/D, CD/1 are enriched with ^{12}C and have $\delta^{13}C_{CH4}$ values below −50 ‰ (Figure 8A). It must be emphasized that methane migrates faster than CO_2 [41], and isotopically lighter methane escapes during excavation. Previous studies concluded that $\delta^{13}C$ values showing a thermogenic isotopic composition are due to CO_2 reduction processes, which was also confirmed by authigenic mineralization (values of $\delta^{13}C_{CaCO3}$ up to 17 ‰) or secondary processes enriching residual methane with ^{13}C. It is also possible that some of the shale-derived gas with thermogenic methane values (<50 ‰) migrated along the Velenje active fault into the main lignite seam (Figure S1). For example, it is known that carbon species from vent fluids from Yellowstone Lake, Wyoming, have multiple sources such as interactions of vent fluids with subsurface rocks and lake sediments are the predominant process, followed by thermal decomposition of organic matter with $\delta^{13}C_{CH4}$ values higher than −50 ‰ [52]. Studies of shale gas have shown that shale gas contains mostly hydrocarbons dominated by methane [53]. Gases produced from most commercially successful shale plays are thermogenic and formations with greater gas endowment contain late-mature thermogenic gas.

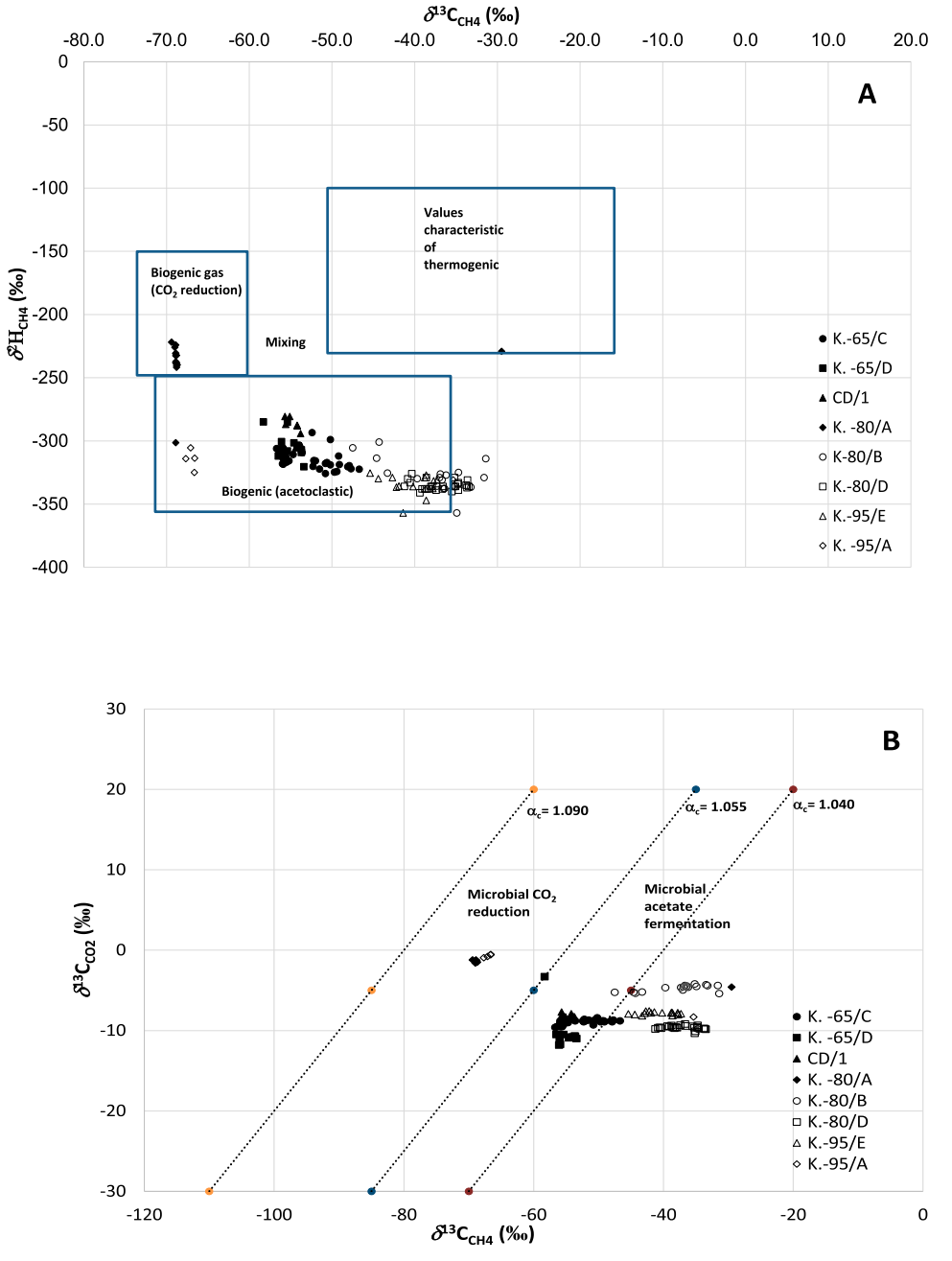

Figure 7. (A) Plot of δ^2H_{CH4} vs $\delta^{13}C_{CH4}$ values in lignite from the Velenje Basin. (B) Plot of $\delta^{13}C_{CO2}$ versus $\delta^{13}C_{CH4}$. The isotope fractionation factors (α_C) are shown for methanogenesis by CO_2 reduction ($1.090<\alpha_C<1.055$) and acetate fermentation ($1.055<\alpha_C<1.040$) derived from [44].

In addition, isotope reversals (δ^{13}C methane > δ^{13}C ethane) are observed in shale plays with mature organic matter that experienced a significant uplift (> 2 km). So far, no studies of gas-derived shales from the Velenje Basin were performed, but it would be

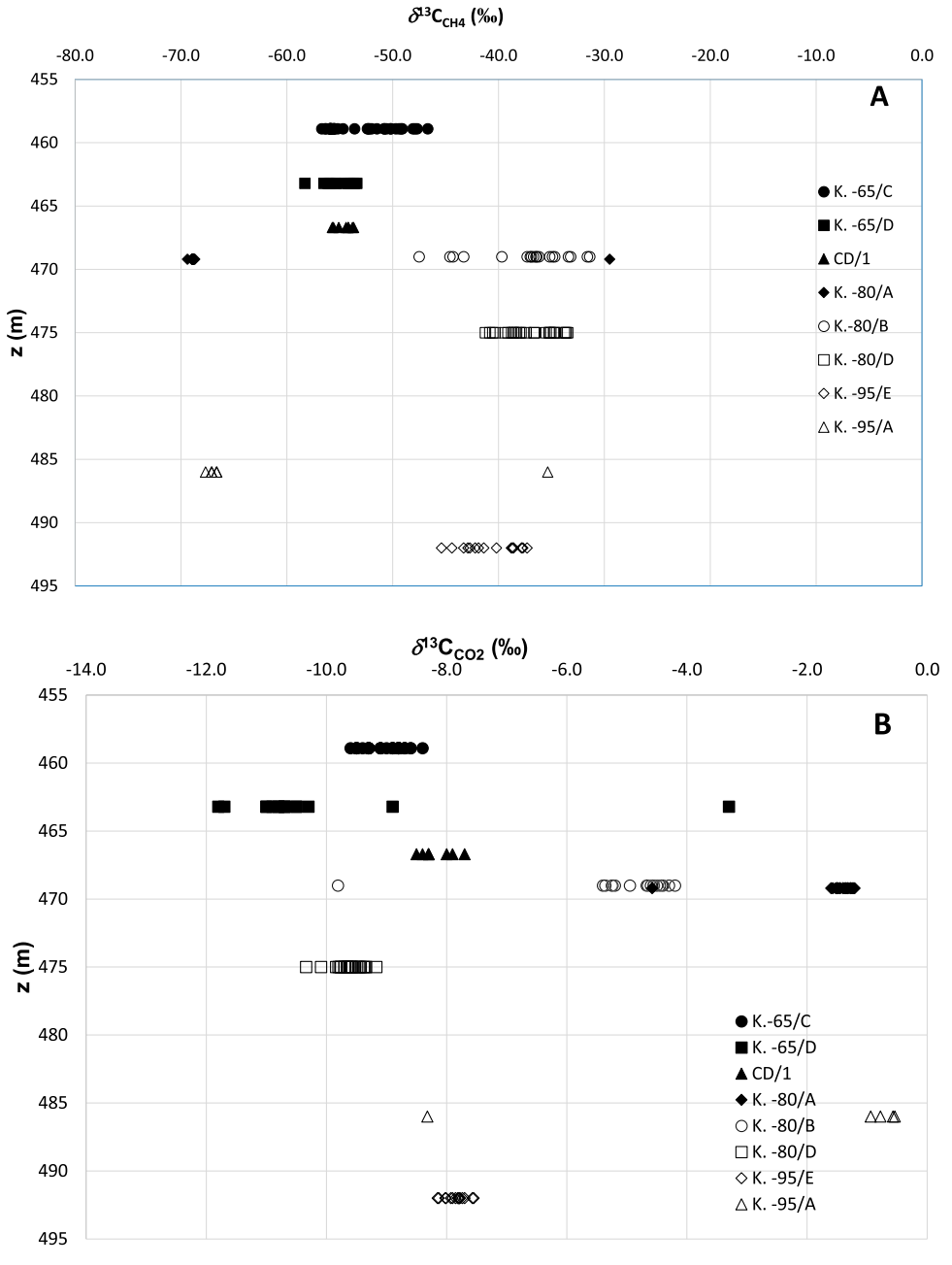

Figure 8. (A) Plot of $\delta^{13}C_{CH4}$ versus depth from K.–65/C (Pesje), K.–65/D (Pesje), CD1 (Preloge), K.–80/A (Pesje), K.–80/B (Pesje), K.–80/D (Pesje), K.–95/E (Pesje), K.–95/A (Pesje). (B) Plot of $\delta^{13}C_{CO2}$ versus depth from K.–65/C (Pesje), K.–65/D (Pesje), CD1 (Preloge), K.–80/A (Pesje), K.–80/B (Pesje), K.–80/D (Pesje), K.–95/E (Pesje), K.–95/A (Pesje).

possible that both gas reservoirs: shales deposited in the Pre – Pliocene basement and the main lignite strata (Figure S1), could be connected along the active Velenje fault and this hypothesis should be tested in the future.

Groundwater also has detectable levels of dissolved methane with isotope values ($\delta^{13}C_{CH4}$ from −77.7 to −51.4 ‰; $\delta^{2}H_{CH4}$ from −274 to −162 ‰) consistent with microbial methanogenesis [36, 37]. These values are comparable to $\delta^{13}C_{CH4}$ values found at excavation fields investigated in this study. The most variation in $\delta^{13}C_{CH4}$ values was observed at K.−80/A, with one sample having a $\delta^{13}C_{CH4}$ value of −29.5 ‰ indicating thermogenic methane (Figure 8 A).

The average $\delta^{13}C_{CO2}$ at investigated excavation fields are as follows: K.-80/A (-1.5 ‰), K.−95/A (−2.2 ‰), K.−80/A (−5.0 ‰), K.−95/E (−7.8 ‰), CD/1 (−8.2 ‰), K.−65/C (−9.0 ‰), K.−80/D (−9.6 ‰), K.−65/D (−10.2 ‰). The $\delta^{13}C_{CO2}$ values are on average −7.8 ‰ and are endogenic in origin (Figure 8 B). Also, higher CDMI values are observed in the range of 95.5–98.3 vol.%. The highest values of $\delta^{13}C_{CO2}$ (−4.6 to −1.2 ‰) were observed at K.-80/A (average $\delta^{13}C_{CO2}$ = −5.0 ‰) indicating a biogenic origin via the CO_2 reduction process (Figure 9B). Higher $\delta^{13}C_{CO2}$ values were observed at K.−95/A, and only one sample had a more negative value (−8.3 ‰) of endogenic CO_2. The shallower excavation fields (K.−65/D and K.−65/C) have the most negative $\delta^{13}C_{CO2}$ values indicating that the CO_2 is biogenic and formed via acetate fermentation (Figure 8 B). A much broader range of $\delta^{13}C_{CO2}$ values (−40 to +25 ‰) was observed in the northern Bowen Basin [51]. Previous studies of the Velenje Basin (G2/C, K.−5/A, K.−130/A and K.−50/C) report $\delta^{13}C_{CO2}$ values from −11 to 5.5 ‰ [26], which is greater than that (−11.8 to −0.54 ‰) reported in this study (Figure 8 B). Excavation fields with fresh overburden have a characteristic low CDMI and a broader range of $\delta^{13}C_{CH4}$ values (−70.0 to −20.0 ‰), while excavations (K.−80/A and K.−95/A) under pre-mined coal have a characteristically high CDMI (Tables 1 and 2).

5.5. PCA analysis

PCA of the coalbed gas shows distinctive groups/clusters (Figure 9). PC1 explains 55.5 % of the variance (positive $\delta^{13}C_{CH4}$ values and negative $\delta^{2}H_{CH4}$ values), while PC2 explains 25.2 % of the variance (positively $\delta^{13}C_{CO2}$ and CDMI). Combined, they account for 80.7 % of the total variance. The most distinct clusters are evident for K.−80/A, where a strong negative relationship exists between $\delta^{2}H_{CH4}$ and $\delta^{13}C_{CO2}$ (group 1 in Figure 9, with K.−95/A). Conversely, K.−95/E has a strong positive relationship between CDMI and $\delta^{13}C_{CH4}$ values (group 3 in Figure 9, with K.−65/C and K.−80/B). K.−80/D is also present in a compact cluster, positively influenced by the $\delta^{13}C_{CH4}$ values, although some overlap with K.−80/B is evident (group 4 in Figure 9 is almost exclusively comprised of K.−80/D).

The data for 151 samples of coalbed gas were then entered into the web-based machine learning tool developed by [22]. The $\delta^{13}C_{CO2}$, $\delta^{13}C_{CH4}$ and $\delta^{2}H_{CH4}$ values were used as input data since higher hydrocarbon concentrations in the Velenje coalbed gas were low [27] and not measured in this study. Measurements of CO_2 and consequently, CDMI values were not included in the machine learning model. Outputs of Milkov's tool are confidence scores (in %) of gas genesis: T – thermogenic, PMCR – primary microbial, PMMF – primary microbial methyl-type fermentation, SM – secondary microbial, A – abiotic) and MA – model accuracy (in %).

Table 3 shows a comparison between hierarchical clustering and machine. The highest percent of equal labeling was observed for boreholes K.−65/C and K.−65/D

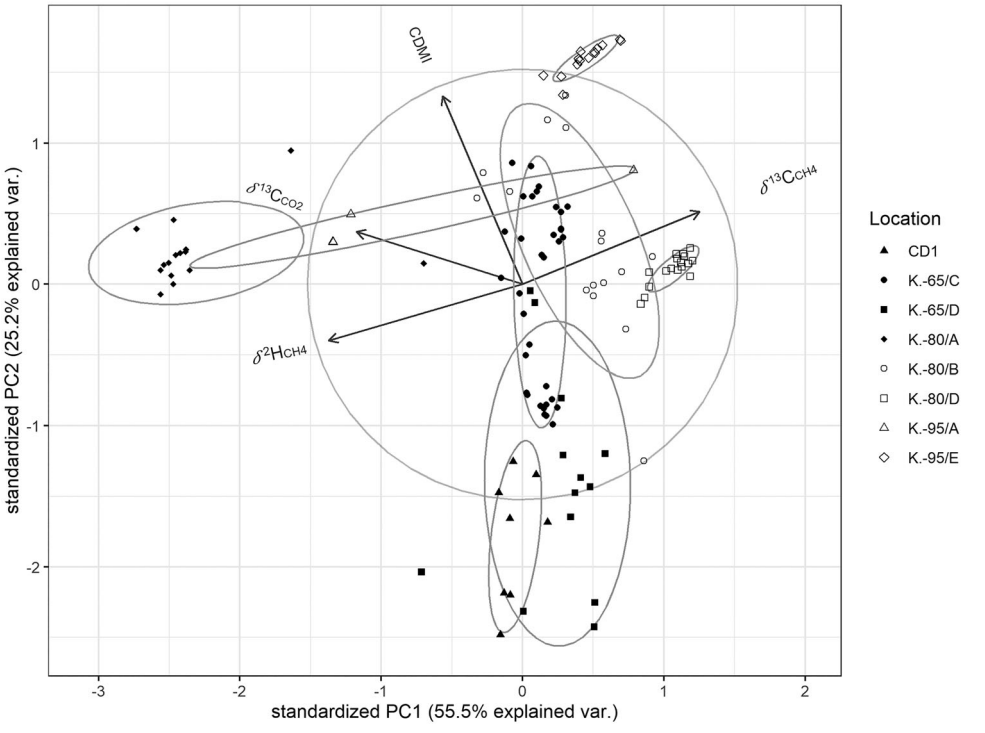

Figure 9. PCA biplot of samples and CDMI, $\delta^{13}C_{CO2}$, $\delta^{13}C_{CH4}$ and $\delta^{2}H_{CH4}$ explanatory variables. Vector sizes indicate the strength of their contribution to each PC. Ellipses (size determined by 0.95 probability) show the observations grouped by location.

with 97.1 and 92.3 vol.%, respectively. The lowest was 6.3 vol.% at K.−80/B. Machine learning predicted that most methane at K.−80/B, K.−80/D and K.−95/E was either abiotic or thermogenic in origin, while hierarchical analysis indicated primary microbial methyl-type fermentation (PMMF) and primary microbial CO_2 reduction (PMCR), which is the leading cause of the low 'same' numbers for these three boreholes.

Hierarchical clustering shows five different groups of coalbed gases in the Velenje indicating that different biogeochemical processes occurred during gas formation (Figure S3).

Table 3. Results from a comparison of hierarchical clustering and a machine learning model. 'Different' indicates where each method's predicted origin differed, while 'Same' indicates where the methods agreed.

Borehole	Different	Same	Total	Percent of same (%)
CD/1	5	3	8	37.5
K.−65/C	1	33	34	97.1
K.−65/D	1	12	13	92.3
K.−80/A	4	11	15	73.3
K.−80/B	15	1	16	6.3
K.−80/D	13	4	17	23.5
K.−95/A	1	3	4	75
K.−95/E	12	2	14	14.3
Total	52	69	121	57

These groups can be characterized as follows:

(1) Dark green: microbial CO_2 reduction (primary microbial CO_2 reduction - PMCR) + endogenic CO_2, high CDMI above 80 vol.% (K.−80/A and K.−95/A),
(2) Brown: microbial acetate fermentation (primary microbial methyl-type fermentation - PMMF), CO_2 reduction, lower CDMI from 50 to 80 vol.% (CD/1, K.−65/C, K.−65/D),
(3) Purple: endogenic CO_2 + acetate fermentation (primary microbial methyl-type fermentation - PMMF), high CDMI above 80 vol.% (K.−95/E, K.−65/C, K.−65/D, K.−80/B),
(4) Pink: endogenic CO_2, acetate fermentation (primary microbial methyl fermentation - PMMF) and CO_2 reduction (primary microbial CO_2 reduction - PMCR), CDMI between 50–80 vol.% (K.−80/D, K.−95/A),
(5) Light green: acetate fermentation (primary microbial methyl-type fermentation -PMMF) and CO_2 reduction (primary microbial CO_2 reduction - PMCR) with CDMI below 25 vol.% (K.−80/B, K.−80/A).

5.6. Spatial distribution of CDMI, $\delta^{13}C_{CO2}$, $\delta^{13}C_{CH4}$, $\alpha_{CO2\text{-}CH4}$

Sampling points and the distribution of measured parameters: CDMI, $\delta^{13}C_{CO2}$, $\delta^{13}C_{CH4}$ and $\alpha_{CO2\text{-}CH4}$ of coalbed gases is presented in Figs. S4, 10 A–D. All data for performing geochemical maps since 2000–2018 are presented in Table S9. In this paper, geochemical maps were updated using 2000–2018 data (Table S9) and presented in a geographical information system (GIS) environment (Figure S4). The maps now contain the new data from three boreholes: JPK83+10° (Pesje K.−80/D), JPK89+10° (Pesje K.−95/E), JPK91+10° (Pesje K.−95/A), while the interpolation maps have been updated with CDMI, $\alpha_{CO2\text{-}CH4}$, $\delta^{13}C_{CO2}$ and $\delta^{13}C_{CH4}$ values. Only the CDMI, $\delta^{13}C_{CO2}$, $\delta^{13}C_{CH4}$ values of the first intact sample from each excavation field were included in the GIS environment. Using the JamTveg GIS [54,55], we interpreted the distribution of gases from the mining areas (active working faces) and their origin, as well as the exit and delivery roadways in Preloge and Pesje mining areas.

From the map, it can be seen that the CDMI values are lower (< 85 vol.%) in the northern part of the Velenje Coal Basin (Figure 10 A). The spatial distribution becomes even more visible on the interpolated map, where higher values (> 85 vol.%) are found in the southern part of the basin close to the Šoštanj fault. The interpolation map is also helpful for determining potential CO_2 gas outburst prone areas, which are located near the Šoštanj fault (Figure 10 A). Higher concentrations of CO_2 and, consequently, higher values of CDMI concerning the active fault zones were observed in the Bowen and Sydney basins [19]. It was also recognized that the strongest rock and gas outbursts occur only in those parts of coal deposits of the Lower Silesian Basin, which are dominated by large amounts of endogenic CO_2 [33]. Therefore, it seems that also in the Velenje Basin, the Šoštanj fault is a significant factor in the migration of CO_2 from some deep-seated source.

The distribution of $\delta^{13}C_{CO2}$ (Figure 10 B) with values from −7.0 to −14.8 ‰ are typical for the degradation of organic matter and are characteristic for all analyzed locations, except in the vicinity of the Šoštanj fault where $\delta^{13}C_{CO2}$ values range from −7.0–4.0 ‰ (Figure 10 B). These higher $\delta^{13}C_{CO2}$ values (up to 4.0 ‰) indicate CO_2 of mixed origin

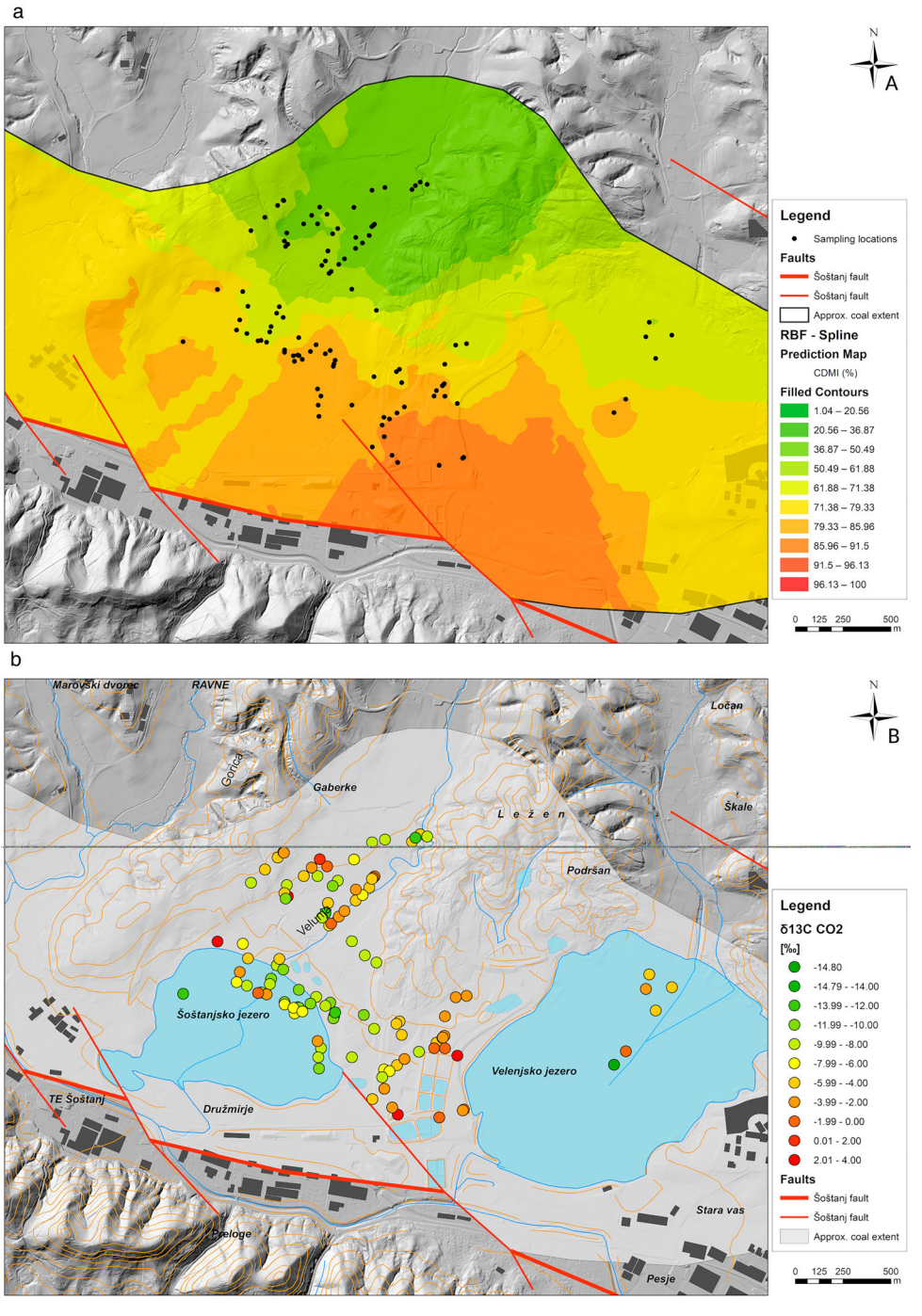

Figure 10. (A) Map showing the carbon dioxide methane index (CDMI) distribution. (B) Map showing the distribution of $\delta^{13}C_{CO2}$ values. (C) Map showing the distribution of $\delta^{13}C_{CH4}$ values. (D). Map showing the distribution of $\alpha_{CO2\text{-}CH4}$ (fractionation factor).

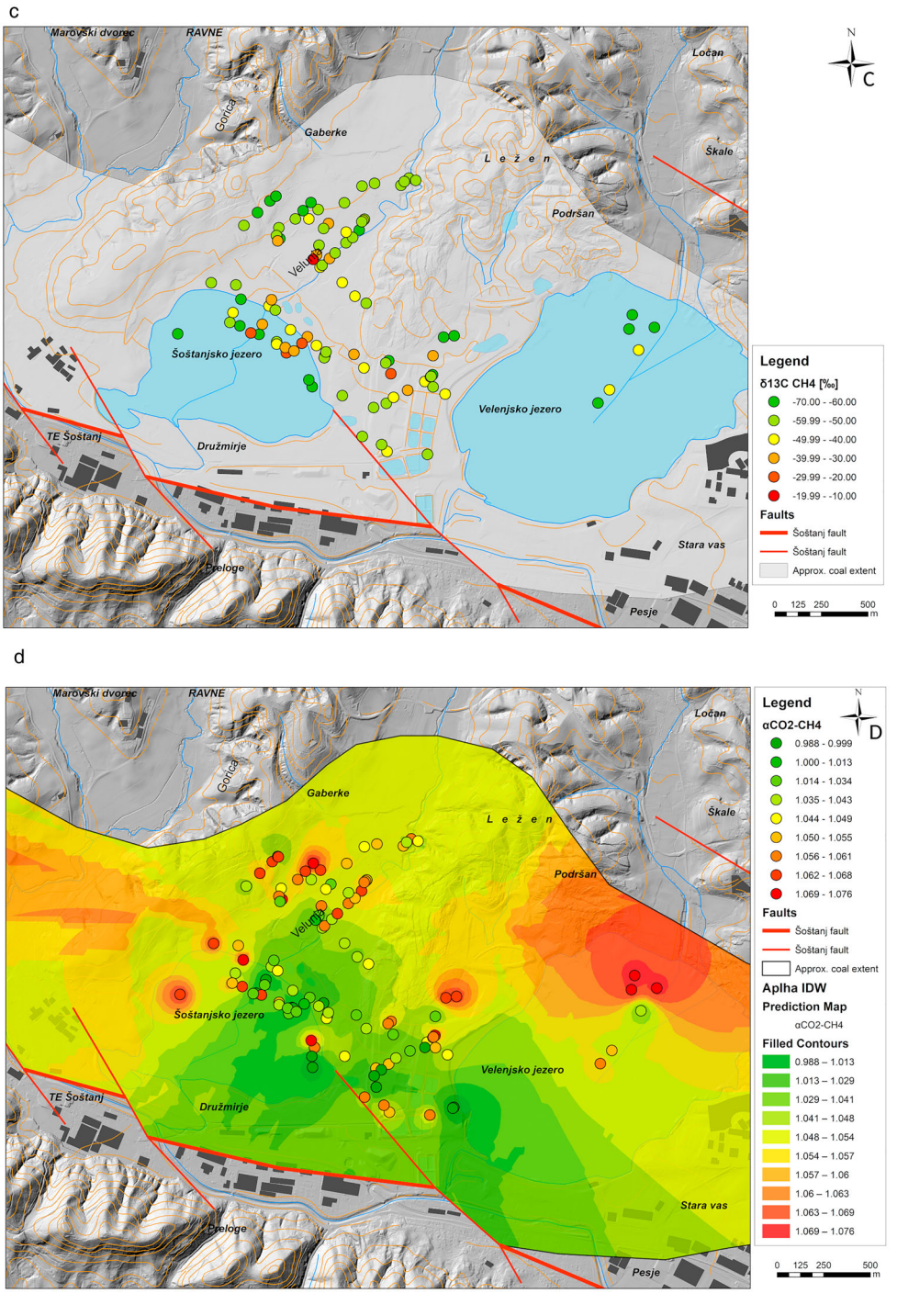

Figure 10 *Continued*

(endogenic and biogenic–CO_2 reduction). Most samples have lower $\delta^{13}C_{CH4}$ values in the range from −74.9 to −50.0 ‰ and indicate gas of bacterial origin (Figure 10 C). The interpolation map of $\alpha_{CO2\text{-}CH4}$ reveals an area with microbial CO_2 reduction ($\alpha_{CO2\text{-}CH4} > 1.055$) and microbial acetate fermentation ($\alpha_{CO2\text{-}CH4} < 1.055$). Microbial CO_2 reduction is a characteristic feature present in the central part of the basin and along the faults, while the eastern, western and northern parts of the basin are characterized by acetate fermentation (Figure 10 D).

6. Conclusion

Molecular (CH_4, CO_2, N_2) and isotopic ($\delta^{13}C_{CO2}$, $\delta^{13}C_{CH4}$, $\delta^{2}H_{CH4}$) compositions were used to better understand the degasification mechanism from eight excavation sites under fresh overburden and pre-mined coal areas at the Preloge and Pesje mining areas in the Velenje Basin from 2013 to 2018. Gas measurements were made in advance of the longwall faces, and the origins of methane and CO_2 were determined. Statistical analysis, including PCA as applied, and geochemical maps for the spatial distribution of coalbed gases were created.

Concentrations of CO_2 prevail at all the investigated excavation fields. Concentrations of CO_2 and methane are related to the position of the working seam in space; generally, two peaks in the levels of CO_2 and methane are observed over fresh burden moving back from the longwall face, while levels of CO_2 and methane under pre-mined coal area remain relatively constant. A decrease in $\delta^{13}C_{CH4}$ values and the diffusive escape of ^{13}C-depleted methane is observed with increasing distance from the longwall face at all investigated excavation fields. More extensive isotope fractionation with distance from the longwall face is observed for $\delta^{13}C_{CH4}$ (2.0–39.9 ‰), while for $\delta^{13}C_{CO2}$ isotope fractionation ranged from 0.6–8.5 ‰.

Shallower excavation fields (K.−65/C, K.−65/D, and CD/1) have $\delta^{13}C_{CH4}$ values $\leq$ -50 ‰, while in the deeper excavation fields 8 K.−95/E, K.−95/A, K.−80/B, and K.−80/D) $\delta^{13}C_{CH4}$ values were $\geq$ −50 ‰. Thus, each excavation field appears to be specific in terms of the geochemical characteristics of coalbed gases, making it necessary to carry out a geochemical and isotope investigation of coalbed gas to understand better the degassing mechanism from excavations, origin of gases, especially methane, which is considered as a greenhouse and unconventional gas.

Statistical analysis revealed five different groups of coalbed gases considering their origin at active excavation fields: (1) microbial CO_2 reduction with high CDMI above 80 vol.%, (2) microbial acetate fermentation with CDMI from 50 to 80 vol.%, (3) endogenic CO_2 and acetate fermentation with CDMI above 80 vol.%, (4) endogenic CO_2, acetate fermentation and CO_2 reduction with CDMI from 50 to 80 vol.%, (5) acetate fermentation and CO_2 reduction with CDMI below 25 vol.%. A comparison of machine learning and hierarchical cluster analysis to decipher the origin of methane found that machine learning is a more useful tool for interpreting the origin of methane in the Velenje Basin. Going forward, it is recommended that CO_2, and CDMI values should be included in machine learning as input parameters in CO_2 rich basins.

The updated interpolated GIS maps reveal that high CDMI, acetate fermentation and endogenic CO_2 are located in the southern part of the Velenje Basin, while in the northeastern part of the basin and some parts of the central basin CO_2 reduction is the major process. The $\delta^{13}C_{CH4}$ and $\delta^{2}H_{CH4}$ values also show that methane is biogenic in origin,

formed by biogenic fermentation and CO_2 reduction processes. Some $\delta^{13}C_{CH4}$ values are also enriched with ^{13}C (i.e. thermogenic methane), which agrees with the previous study of authigenic carbonate mineralization, and high $\delta^{13}C_{CaCO3}$ values (up to 17 ‰) suggest that CO_2 reduction is the primary biogeochemical process, which gives higher $\delta^{13}C_{CH4}$ values. Such investigations (monitoring of molecular and isotopic compositions at excavation fields) are relevant for the safety of coal miners and possible development of clean coal technologies, e.g. coalbed methane (CBM) once the excavation of coal has ceased.

Acknowledgements

We thank Dr Arkadije Popović and Stojan Žigon for performing coalbed gases (CO_2, CH_4, N_2, O_2) measurements. The authors are grateful to Velenje Coal Mine d.o.o., which provided the necessary assets for coalbed gas collection in the last 20 years. Thanks to an external reviewer who helped improve the article.

Disclosure statement

No potential conflict of interest was reported by the authors.

Funding

The authors acknowledge financial support from the state budget by the Slovenian Research Agency (research programmes: L1-5451, P1-0143 and P1-0195). In addition, the authors are grateful to the MASSTWIN-H2020 Twining project: Spreading Excellence and Widening Participation in Support of Mass Spectrometry and Related Techniques in Health, Environment and Food Analysis (Grant Agreement No. 692241).

References

[1] Smith JW, Pallaser R, Pang LSK. Thermal reactions of acetic acid:$^{13}C/^{12}C$ partitioning between CO_2 and CH_4. Org Geochem. 1996;29:79–82.
[2] Stach E, Mackowsky M-T, Teichmüller M, et al. Stach's textbook of coal petrology. Berlin: Gebrüder Borntraeger. 1982.
[3] Milkov AV, Etiope G. Revised genetic diagrams for natural gases based on a global dataset of (20,000 samples. Org Geochem. 2018;125:109–120.
[4] Kotarba M. Isotopic geochemistry and habitat of the natural gases from the Upper Carboniferous Zacler coal-bearing formation in the Nowa Ruda coal district (Lower Silesia. Poland). Org Geochem. 1990;16:549–560.
[5] Kroos BM, Littke R, Müller B, et al. Generation of nitrogen and methane from sedimentary organic matter: implication on the dynamics of natural gas accumulations. Chem Geol. 1995;126:291–318.
[6] Milkov AV. Worldwide distribution and significance of secondary microbial methane formed during petroleum biodegradation in conventional reservoirs. Org Geochem. 2011;42:184–207.
[7] Patience RL. Where did all the coal gas go? Org Geochem. 2003;34:375–387.
[8] Faramawy S, Zaki T, Sakr AAE. Natural gas origin, composition, and processing: A review. J Nat Gas Sci Eng. 2016;34:34–54.
[9] Berner RA. Early diagenesis–A theoretical approach. New Jersey: University Press Princeton; 1980. (Princeton Series in Geochemistry; 1).
[10] Appelo CAJ, Postma D. Geochemistry, groundwater and pollution. 2nd ed Rotterdam: A.A. Balkema Publishers; 1994.

[11] Woese CR, Kandler O, Wheelis ML. Towards a natural system of organisms: proposal for the domains Archaea, Bacteria, and Eucarya. Proc Natl Acad Sci USA. 1999;87:44576–44579.
[12] Whiticar MJ, Faber E, Schoell M. Biogenic methane formation in marine and freshwater environments: CO_2 reduction vs. acetate fermentation–isotopic evidence. Geochim Cosmochim Acta. 1986;50:693–709.
[13] Strąpoć D, Ashby M, Wood L, et al. Significant contribution of methyl/methanol-utilizing methanogenic pathway in a subsurface biogas environment. In: Whitby C, Skovhus TL, editors. Applied microbiology and molecular biology in oil field systems. Dordrecht: Springer; 2010. p. 211–216.
[14] Strąpoć D. Biogenic methane. In: White WM, editor. Encyclopedia of geochemistry. Cham: Springer International Publishing; 2017. p. 9.
[15] Schoell M. Genetic characterization of natural gases. Am Assoc Pet Geol Bull. 1983;67:2225–2238.
[16] Clark I, Fritz P. Environmental isotopes in hydrology. New York (NY): Lewis Publishers; 1997.
[17] Etiope G, Schoell M. Abiogenic gas: atypical but not rare. Elements. 2014;10:291–296.
[18] Javoy M, Pineau F, Delarme H. Carbon and nitrogen isotopes in the mantle. Chem Geol. 1986;57:41–62.
[19] Flores RM. Coalbed methane: from hazard to resource. Int J Coal Geol. 1998;35:3–26.
[20] Cao Y, Davis A, Liu R, et al. The influence of tectonic deformation on some geochemical properties of coals–a possible indicator of outburst potential. Int J Coal Geol. 2003;53(2):69–79.
[21] Smith JW, Gould KW. An isotopic study of the role of carbon dioxide in outbursts in coalmines. Geochem J. 1980;14:27–32.
[22] Snodgrass JE, Milkov AV. Web-based machine learning tool that determines the origin of natural gases. Comput Geosci. 2020;145:104595.
[23] Markič M, Sachsenhofer RF. Petrographic composition and depositional environments of the Pliocene Velenje lignite seam (Slovenia). Int J Coal Geol. 1997;33:229–254.
[24] Markič M, Sachsenhofer RF. The Velenje lignite–Its petrology and genesis. Ljubljana (LJ): Geološki zavod Slovenije; 2010.
[25] Brezigar A. [Coal seam of the Velenje coal mine]. Geologija. 1987;28:319–336. Slovene with English summary.
[26] Pleničar M, Ogorelec B, Novak M. Geologija slovenije = Geology of Slovenia. Ljubljana: Geological Survey of Slovenia; 2009.
[27] Lazar J, Kanduč T, Jamnikar S, et al. Distribution, composition and origin of coalbed gases in excavation fields from the Preloge and Pesje mining areas, Velenje Basin, Slovenia. Int J Coal Geol. 2014;131:363–377.
[28] Kanduč T, Pezdič J, Lojen S, et al. Study of the gas composition ahead of the working face in a lignite seam from the Velenje basin. RMZ Mater Geoenviron. 2003;50:503–511.
[29] Kanduč T, Žula J, Zavšek S. Tracing coalbed gas dynamics and origin of gases in advancement of the working faces at mining areas Preloge and Pesje. Velenje Basin. RMZ Mater Geoenviron. 2011;58:273–288.
[30] Kanduč T, Zavšek S, Jamnikar S, et al. Spatial distribution and origin of coalbed gases at the working faces of the Velenje coal basin, Slovenia, since the year 2000. RMZ Mater Geoenviron. 2016;63(4):213–225.
[31] Kanduč T, Pezdič J. Origin and distribution of coalbed gases from the Velenje basin Slovenia. Geochem J. 2005;39:397–409.
[32] Kanduč T, Markič M, Zavšek S, et al. Carbon cycling in the Pliocene Velenje coal basin, Slovenia, inferred from stable carbon isotopes. Int J Coal Geol. 2012;89:70–83.
[33] Kanduč T, Grassa F, Lazar J, et al. Geochemical and isotopic characterization of coalbed gases in active excavation fields at Preloge and Pesje mining areas. RMZ Mater Geoenviron. 2015;62:21–35.
[34] Kotarba MJ, Rice DD. Composition and origin of coalbed gases in the Lower Silesian basin, southwest Poland. Appl Geochem. 2001;16(7–8):895–910.
[35] Kanduč T, Vreča P, Gregorin Š, et al. Authigenic mineralization in low-rank coals from the Velenje Basin, Slovenia. J Sediment Res. 2018;88(2):201–213.

[36] Kanduč T, Grassa F, McIntosh J, et al. A geochemical and stable isotope investigation of groundwater/surface water interactions from the Velenje Basin, Slovenia. Hydrogeol J. 2014;22(4):971–984.
[37] Kanduč T, Šlejkovec Z, Vreča P, et al. The effect of geochemical processes on groundwater in the Velenje coal basin, Slovenia: insights from mineralogy, trace elements and isotopes signatures. SN Appl Sci. 2019;1:1518.
[38] Coplen TB. New guidances for reporting stable hydrogen, carbon and oxygen isotopes ratio data. Geochim Cosmochim Acta. 1996;60:390–3360.
[39] Petroleum geochemistry group, CSIRO [Internet]. Gas composition and isotope geochemistry. [cited 6/12/2000]. Available from: http://www.dpr.csiro.au/research/erp/gcig.html
[40] Kotarba MJ. Composition and origin of coalbed gases in the Upper Silesian and lublin basins, Poland. Org Geochem. 2001;32:163–180.
[41] Atkins PW. Physical chemistry. 5th ed Oxford: Oxford University Press; 1994.
[42] Grassa F, Capasso G, Oliveri Y, et al. Nitrogen isotopes determination in natural gas: analytical method and first results on magmatic, hydrothermal and soil gas samples. Isot Environ Health Stud. 2010;46(2):141–155.
[43] Brand WA, Coplen TB, Vogl J, et al. Assessment of international reference materials for isotope-ratio analysis (IUPAC technical report). Pure Appl Chem. 2014;86(3):425–467.
[44] Schoell M. Multiple origins of methane in the earth. Chem Geol. 1998;71(1–3):1–10.
[45] R Core Team R [Internet]. A language and environment for statistical computing. R Foundation for Statistical Computing, Vienna, Austria. [updated: 27.8.2020 cited: 27.8.2020]. Available from:https://www.R-project.org/; 2019.
[46] Wickham H. Ggplot2: elegant graphics for data analysis. New York (NY): Springer; 2016.
[47] Snodgrass JE, Milkov AV. Web-based machine learning tool that determines the origin of natural gases. Comput Geosci. 2020;145:104595.
[48] Beamish BB, Crosdale PJ. Instantaneous outbursts in underground coal mines: An overview and association with coal type. Int J Coal Geol. 1998;35(1–4):27–55.
[49] Završek S, Markič M, Vrabec M, et al. Poročilo o raziskavah lokacije izbruha plina v odvozni progi et.k.–90C [Report on the research of gas outburst locations in the exit roadways K.–90C]. Velenje: Premogovnik Velenje; 2003. Slovene.
[50] Rice DD. Composition and origin of coalbed gas. In: Law BE, Rice DD, editor. Hydrocarbons from coal. Tulsa, OK: American Association of Petroleum Geologists; 1993. p. 159–184. (AAPG Studies in geology; 38).
[51] Golding SD, Boreham CJ, Esterle JS. Stable isotope geochemistry of coalbed and shale gas and related production waters: A review. Int J Coal Geol. 2013;120:24–40.
[52] Ong C, Fowler APG, Seyfried Jr. WE, et al. Organic compounds in vent fluids from Yellowstone lake, wyoming. Org Geochem. 2021;159:104275.
[53] Milkov AV, Faiz M, Etiope G. Geochemistry of shale gases from around the world: composition, origins, isotope reversals and rollovers, and implications for the exploration of shale plays. Org Geochem. 2020;143:103997.
[54] Verbovšek T. Jamtveg GIS (software equipment). Ljubljana: Natural Science Faculty, Department of Geology; 2010; Slovene.
[55] Verbovšek T, Vrabec M. Jamtveg GIS (software equipment). 2nd ed. Ljubljana: Natural Science Faculty, Department of Geology; 2012. Slovene.